https://doi.org/10.1016/j.enconman.2019.111963
This is the Pre-Published Version.

Advanced Exergy Analysis of Organic Rankine Cycles for Fischer-Tropsch Syngas Production with Parallel Dry and Steam Methane Reforming

Chenglei Yan[a,b], I-Lung Chien[c], Shun'an Wei [a,b], Weifeng Shen [a,b,*], and Jingzheng Ren[d,*]

[a]School of Chemistry and Chemical Engineering, Chongqing University, Chongqing 400044, P. R. China

[b]National-municipal Joint Engineering laboratory for Chemical Process Intensification and Reaction, Chongqing University, Chongqing 400044, China

[c]Department of Chemical Engineering, National Taiwan University, Taipei 10617, Taiwan

[d]Department of Industrial and Systems Engineering, The Hong Kong Polytechnic University, Hong Kong SAR, China

Corresponding Author: *(W.S) E-mail: shenweifeng@cqu.edu.cn, *(J.R) E-mail: jzhren@polyu.edu.hk

Abstract: The process for producing Fischer-Tropsch syngas (FTS) with the combination of steam and dry methane reforming (operating in parallel), is demonstrated with the most favorable economics. The locations and degrees of the inefficiency in the process are studied based on the conventional exergy analysis (CEA). The advanced exergy analysis (AEA) is further applied to evaluate the energy-saving potential of each equipment and thermodynamic interactions among them. After these, the optimized ORCs with (or without) recuperators are introduced to recovery the waste heat according to the obtained exergy analysis results. The thermodynamic efficiency and total exergy destruction of the ORCs are defined as the objective function to determine the most appropriate working fluids and obtain optimal operation conditions. The performances of proposed three different ORC schemes are also assessed, and the dual-pressure ORC system has the best performance with highest thermal efficiency accounting to 15.39%, annual net profit (ANP) accounting t 1.55 E+07$.year^{-1} and 4.6 years payback period. The exergy loss of the novel system integrating with the dual-pressure ORC scheme is

© 2019. This manuscript version is made available under the CC-BY-NC-ND 4.0 license http://creativecommons.org/licenses/by-nc-nd/4.0/

reduced to 13.21 MW while the exergy loss in the previous process accounts to 34.92 MW, and 88.21% of avoidable endogenous exergy destructions are recovered from waste heat sources. The proposed energy conservation approach in this study can be extended to some other similar chemical processes for achieving the maximum exergy- and energy-savings.

Keywords: Fischer-Tropsch syngas; Advanced exergy analysis; Organic Rankine Cycles; Optimization

Nomenclature

AEA	Advanced exergy analysis
ANP	Annual Net Profit, $/year
AP	Annual profit, $/year
ATR	Auto-thermal Reforming
CEA	Conventional exergy analysis
DMR	Dry Methane Reforming
E	Exergy, MW
FTS	Fischer-Tropsch syngas
GTL	Gas to Hydrocarbon Liquids
H	Enthalpy, kJ/mol
I	Fraction interest rate
m	Mass flow rate, kg/h
n	Number of years
NPV	Net present value
ORC	Organic Rankine Cycle
P	Pressure, kPa
PR	Peng-Robinson
Q	Heat duty, kW
S	Entropy, kJ/(mol. K)
SMR	Steam Methane Reforming
T	Temperature, K
TAC	Total annualized cost, $/year

WGS	Water gas shift
Subscripts	
AV	Avoidable
D	Destruction
EN	Endogenous
EX	Exogenous
UN	Unavoidable
F	Feed
P	Product
k	k-th equipment
i	Component i
In	Input
Out	Output
p	Isobaric condition
0	Reference condition
Superscripts	
CH	Chemical
PH	Physical
Greek letters	
η	Exergy efficiency

1. Introduction

Abundant supplies of natural gas have stimulated interest in increasing the use of natural gas for both power and chemicals production. The nature gas based Fischer-Tropsch synthesis (FTS) process is considered as one of the most promising alternative-to-petroleum technologies to produce liquid hydrocarbons for fuels and chemicals [1, 2]. The appropriate concentrations of each content (*e.g.*, CO, H_2, CO_2, CH_4, and H_2O) in the syngas are required to improve the yields of hydrocarbon. The amount of CO_2 and CH_4 should be as low as practicable to improve the conversion of the CO [3], and the suitable H_2/CO ratio of the syngas should be as close as possible to the value 2.

Many studies [4-7] explored the economic performances of several alternative chemical processes including combinations of steam methane reforming (SMR), dry methane reforming (DMR), auto-thermal reforming and gas heated reforming for FTS. The SMR process is a major syngas production process for Fischer-Tropsch production [8, 9]. However, the synthesis gas produced based on SMR could not be directly utilized for FTS process due to the high H_2/CO ratio (>3). Therefore, DMR process that generates syngas with a low H_2/CO ratio (<1) was proposed to combine with SMR [10]. The economic comparison of several alternative processes for producing FTS was explored Luyben *et al*. [11, 12], and the investigation demonstrated that the process composed of SMR and DMR operating in parallel provided the best economic performance, this process was thereby a research focus in this study. Rezaei and Dzuryk [13] also found that syngas production processes by the DMR reaction and its combination with the SMR reaction have greater economics of reverse water gas shift (RWGS) reaction.

To reduce the consumption of fossil fuels and mitigate negative environment impacts, it is important to pursue the efficient energy utilization in the energy-intensive chemical process. As an effective approach to analyze and evaluate the irreversible thermodynamics of a chemical process, the advanced exergy analysis (AEA), splits the exergy destruction of each equipment into avoidable or unavoidable and endogenous or exogenous parts [14]. AEA can evaluate thermodynamic interactions between equipments in the whole system and quantify the real improvement potential by overcoming the limitation of the conventional exergy analysis (CEA). The study of irreversibility and exergy destruction of five conventional mixed natural gas liquefaction processes was carried out by Vatani *et al*. [15] based on the AEA, and they found that improving the exergy efficiency of an equipment could reduce the exergy destruction of other equipments which have interactions with. Yang et al. [16] explored the energy-saving potential in an oil shale retorting process using AEA. The strategy was also studied by Mehrpooya et al. [17] for evaluating the process performance of the ethane recovery plant, and they demonstrated that the exergy destructions of the overall process were majorly lost in unavoidable parts while the compressors had the highest irreversibility in endogenous

and avoidable parts. According to the AEA, Penkuhn and Tsatsaronis [18] evaluated two different configurations in determining the real improvement potential in ammonia synthesis.

On the other hand, it also has great significance to improve the energy utilization efficiency of a chemical process by integrating with some specific strategies including Organic Rankine Cycle (ORC) [19]. ORC utilizes medium- and low-grade heat sources to generate electrical power using the organic fluid as working medium [20]. There are large amount of low-grade waste heats existing in the chemical process industry (*e.g.,* refinery plant) that are difficult to be used due to the diversity of the forms, process restriction, and temperature limitation. Pierobon et al. [21] applied the ORC to recover the waste heat from the SGT-500 gas turbine, and the generated electrical power was supported to the Draugen off-shore platform. The investigation and comparison between the CO_2 transcritical electrical power cycle and the R245fa ORC were investigated by Li et al. [22] and they found that the exergy efficiency of the R245fa ORC were slightly higher than those in CO_2 transcritical power cycle when the operation condition was kept at the same. Yu et al. [23] proposed a model for the optimization of the ORC process in refineries. After this, Yu et al. [24] reported a novel method to optimize the ORC system by determining the working fluid and operating conditions. Meanwhile, the required optimal operation conditions of the ORC were proposed to recover the waste heat completely and generating the maximum electrical power output. Inspired by above studies, this study aims to extend the ORC techniques to the FTS syngas production processes for achieving higher energy efficiency.

In this study, the conventional and advanced exergy analysis were employed to investigate the existing syngas production process with heat integration, and the ORCs were optimized for waste heat recovery. The exergy destructions of each equipment are explored based on the CEA, which provides the information regarding the location and magnitude of the inefficiencies in the overall process. The AEA is further used to evaluate the thermodynamic interactions among different equipments and reveal the real improvement potentials of each equipment. Based on the above-mentioned results, the ORCs with (or without) recuperators are applied. The

comparison on three preselected working fluids (*i.e.,* isopentane, N-pentane, and N-hexane) are investigated to obtain the optimum working fluids. The evaporator inlet temperature and turbine outlet pressure are also optimized by considering the system thermal efficiency and total exergy destruction of the ORC as the objective functions. Moreover, three schemes for recovering energy from sensitive waste heat sources in the syngas production process by integrating with optimal multiplied ORCs are proposed and evaluated.

2. Process description

2.1 Fischer-Tropsch syngas production process combining DMR and SMR

The schematic diagram of the combined SMR and DRM in parallel for Fischer-Tropsch (FT) process with heat integration is illustrated in Fig. 1. The existing process with an amount of syngas product (*i.e.,* 15000 kmol/h H_2 and 7500 kmol/h CO) is set based on Baltrusaitis and Luyben [11, 12]. The reactions involved in SMR and DRM are assumed to achieve chemical equilibrium at high operation temperature. The RGibbs reactor model based on the minimum free energy is selected.

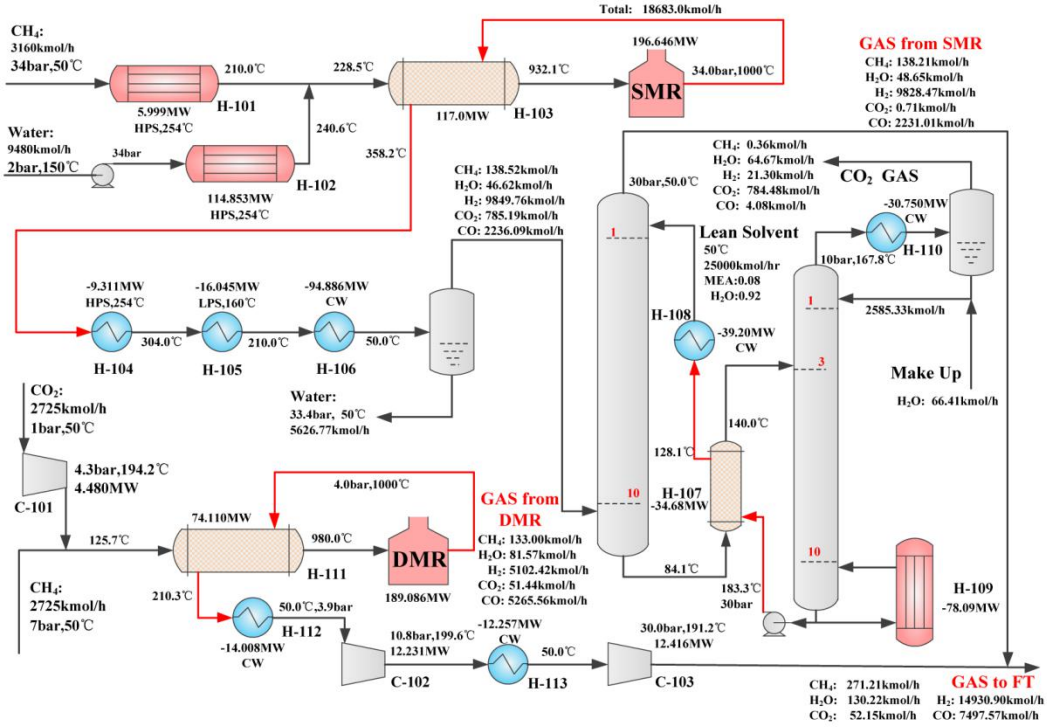

Fig. 1 The existing process for producing Fischer-Tropsch syngas with parallel SMR and DRM.

(1) SMR/DRM processes

The widely applied SMR process is composed of two reactions involving methane reforming and water gas shift (WGS), which is the summation of reaction 1 and 2:

$$CH_4 + H_2O \Leftrightarrow CO + 3H_2 \quad (1)$$

$$CO + H_2O \Leftrightarrow CO_2 + H_2 \quad (2)$$

The alternative to steam methane reforming for the production of syngas is DMR process with carbon dioxide as the raw material. The methane is reacted with carbon dioxide, and the reaction is described as follow:

$$CH_4 + CO_2 \Leftrightarrow 2CO + 2H_2 \quad (3)$$

The two parallel reaction systems are both operated at high reaction temperature (1000 ℃) to achieve a higher methane conversion. The operation pressures of SMR and DRM reactors are required at 34 bar and 4 bar, respectively. The feed to the SMR consists of 3160 kmol/h of methane and 9480 kmol/h of water. In addition, flow rates of the feed including methane and carbon dioxide to DRM are both 2725 kmol/hr. To fully use the energy from overall system, hot reactor effluents with the temperature of 1000 ℃ from both SMR and DRM are employed to preheat their respective fresh stream to 932 ℃ (fed to SMR) and 980 ℃ (fed to DMR) in the feed-effluent heat exchanger. The hot gas from the SMR reactor effluent is cooled in a series of heat exchangers. The high-pressure and low-pressure steam at 254 ℃ and 160 ℃ is generated by H-104 and H-105, respectively, before the gas is cooled down to 50 ℃ in H-106 by cooling water. Liquid water is removed in the separator drum and the gas is fed to the CO_2 absorber. The hot gas from the DMR reactor effluent is also cooled to 50 ℃ and sent to a two-stage compression system.

(2) CO_2 Capture Process

The existing MEA-based CO_2 capture process [25] consists of a CO_2 absorber and a stripper as described in Fig. 1. The syngas gas with mole fractions of 6.01% CO_2, 0.35% H_2O, 17.13% CO, 1.06% CH_4 and 75.45% H_2 is fed to the bottom of the absorber. The upgraded syngas is gathered at the top of absorber where the raw syngas sufficiently react with 25000 kmol/h MEA solution (8mol% MEA and

92mol% water) in the counter-current direction. The rich MEA solvent from the bottom of the absorber is preheated by lean MEA through a lean/rich cross heat exchanger and then be fed to the 3rd stage of the desorption column. The stripper overhead stream is cooled by a condenser with the operation condition of 90 ℃ and 10 bar. The cooling water combined with the makeup MEA solution as the reflux is returned to the top of stripper. Meanwhile, the external steam supplies the heat to the reboiler at the bottom of stripper for the regenerating of the lean MEA solution which is recycled back to the absorber. The removed gas (mainly CO_2) can be recycled as the feed of the DMR process.

2.2 Organic Rankine cycle (ORC) process

The ordinary ORC system [26] involving an evaporator, a turbine, a condenser and a pump is illustrated in Fig. 2(a). Operationally, the energy from the low-grade waste heat source is supplied to the evaporator in the ORC system. As a result, the organic working fluid with lower boiling temperature is vaporized or even super-heated (points 5 and 1) in the evaporator. The saturated or super-heated vapor with high temperature and high pressure is expanded in the turbine (point 2) to produce the electricity power by an electrical generator. Afterwards, the expanded vapor with low pressure is slightly subcooled into saturated liquid in the condenser (point 4). Eventually, the working fluid is pressurized by the pump and recycled to the evaporator (point 5). In order to improve the thermal efficiency of the ORC, the ORC with the recuperator installing between stream 5 and 6 is proposed, as is evident in Fig. 2(b). The application of the recuperator is expected to preheat the cooling working fluid (point 5) and desuperheat the exhausted vapor (point 5) for further energy utilization.

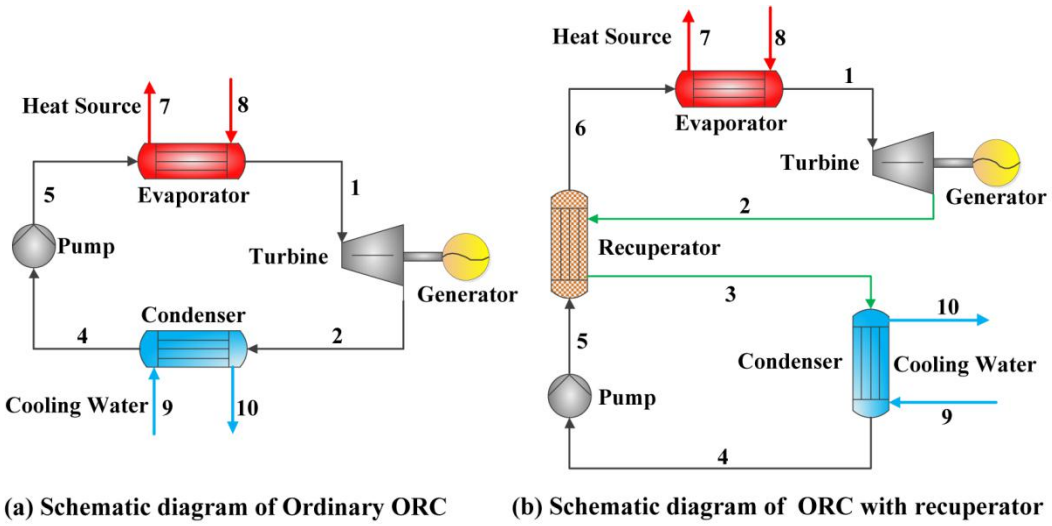

Fig. 2 (a) Schematic diagram of ordinary ORC; (b) Schematic diagram of ORC with an additional recuperator.

3. Methodology

3.1 Conventional exergy analysis

The concept of exergy is used to evaluate the irreversibility of the systematic process based on the first and second laws of the thermodynamics. By neglecting the effects of kinetic, potential and nuclear energies, the total exergy E^{Total} can be divided into two parts of chemical E^{CH} and physical exergy E^{PH}, and it can be calculated by Eq. (4).

$$E^{Total} = E^{PH} + E^{CH} \tag{4}$$

The chemical exergy is the maximum theoretical useful work obtainable as the system passes from the restricted dead state to the dead state where it is in complete equilibrium with the environment. The chemical exergy of a stream is the sum of the standard exergy of each component multiplied by their mole fractions [27]. The physical exergy of a flow is known as the maximum theoretical work possible from that flow, under the conditions of exchanging heat only with its surrounding, following which the flow is brought back to the pressure and temperature of the environment. The reference state of the environment in this study is defined as 25 ℃ and 1.013 bar based on the study of Szargut *et al.* [28]. The physical exergy can be determined by Eq. 5:

$$E^{PH} = (h - h_0) - T_0(S - S_0) \tag{5}$$

where T_0 and S are enthalpy and entropy of the flow at working condition, respectively. T_0 is the surrounding temperature. h_0 and S_0 are enthalpy and entropy of the flow under environment conditions, respectively.

The exergy balance of a system is investigated to analyze the degradation of energy by calculating the exergy value of every input or output stream [29]. The exergy destruction indicating the loss in energy quality for an open thermodynamic system is expressed as follow:

$$\dot{E}_{D,tot} = \dot{E}_{F,tot} - \dot{E}_{P,tot} \tag{6}$$

where, $\dot{E}_{D,tot}$, $\dot{E}_{F,tot}$, and $\dot{E}_{P,tot}$ represent the exergy destruction, the input exergy, and the output exergy of the overall system, respectively.

To explore the exergy loss distribution of the overall system, the exergy destruction of each equipment should be initially calculated. The exergy destruction rate $\dot{E}_{D,k}$ within the k-th equipment is calculated as the difference between the exergy rate of feed $\dot{E}_{F,k}$ and the exergy rate of product $\dot{E}_{P,k}$ based on the exergy balance:

$$\dot{E}_{D,k} = \dot{E}_{F,k} - \dot{E}_{P,k} \tag{7}$$

In order to assess the utilization of the energy and exergy, two variables including exergy efficiency (ε) and exergy destruction ratio (y) are adopted to evaluate the performance of a thermal system as follows:

$$\varepsilon_{Tot} = \frac{\dot{E}_{P,tot}}{\dot{E}_{F,tot}} = 1 - \frac{\dot{E}_{D,tot}}{\dot{E}_{F,tot}} \tag{8}$$

$$\varepsilon_k = \frac{\dot{E}_{P,k}}{\dot{E}_{F,k}} = 1 - \frac{\dot{E}_{D,k}}{\dot{E}_{F,k}} \tag{9}$$

Meanwhile, three types of the exergy destruction ratio (y_k, y_k^*, y_{tot}^*) are used to evaluate the contribution of exergy destruction in the whole system with several equipments [30, 31]. These ratios can be defined as:

$$y_k = \frac{\dot{E}_{D,k}}{\dot{E}_{F,tot}} \times 100\% \tag{10}$$

$$y_k^* = \frac{\dot{E}_{D,k}}{\dot{E}_{D,tot}} \times 100\% \tag{11}$$

$$y_{tot}^{*}=\frac{\dot{E}_{D,tot}}{\dot{E}_{F,tot}}\times 100\% \tag{12}$$

where y_k , y_k^* , and y_{tot}^* represent the ratio of exergy destruction within kth equipment to total exergy input of the system, the ratio of exergy destruction within kth equipment to total exergy destruction of the system, and the ratio of total system exergy destruction to total fuel, respectively.

3.2 Advanced exergy analysis

The conventional exergy analysis (CEA) cannot analyze the root of irreversibility. Based on the CEA, AEA [32] is proposed to provide the thermodynamic interactions among the equipments and evaluating the real improving potentials of each equipment. The exergy destruction of each equipment is divided into endogenous and exogenous parts or avoidable and unavoidable parts.

On the one hand, the total exergy destruction within the kth equipment is divided into the endogenous and exogenous parts [33] as shown in Eq. (13):

$$\dot{E}_{D,k}=\dot{E}_{D,k}^{EN}+\dot{E}_{D,k}^{EX} \tag{13}$$

Herein, $\dot{E}_{D,k}^{EN}$ is the endogenous exergy destruction, associated with the kth equipment being considered operates with its current efficiency ε_k when all other equipments operate in an ideal way. In contrast, the exogenous part $\dot{E}_{D,k}^{EX}$ is defined as the exergy destruction within the k-th equipment occurring by the inefficiencies within other equipments.

On the other hand, AEA divide the exergy destruction of the kth equipment into avoidable or unavoidable parts as follow [34]:

$$\dot{E}_{D,k}=\dot{E}_{D,k}^{AV}+\dot{E}_{D,k}^{UN} \tag{14}$$

The $\dot{E}_{D,k}^{UN}$ is the unavoidable exergy destruction, which indicates that the exergy destruction of the kth equipment cannot be reduced due to the technical or economical limitations (*e.g.* availability and costs of materials and manufacturing methods). The avoidable exergy destruction of kth equipment $\dot{E}_{D,k}^{AV}$ is the difference between the total exergy destruction and the unavoidable exergy destruction, which represents the potential reductions in exergy destruction for each equipment.

As a consequence of definitions in Eqs. (13) and (14), the exergy destruction rate

within a equipment k can be described as:

$$\dot{E}_{D,k} = \dot{E}_{D,k}^{EN,AV} + \dot{E}_{D,k}^{EN,UN} + \dot{E}_{D,k}^{EX,AV} + \dot{E}_{D,k}^{EX,UN} \tag{15}$$

where the $\dot{E}_{D,k}^{EN,AV}$ represents the avoidable part of the endogenous exergy destruction within kth equipment, it is can be reduced by optimizing the operation condition of the kth equipment. The $\dot{E}_{D,k}^{EN,UN}$ is the unavoidable portion of the endogenous irreversibility generation in the kth equipment because of the technical or economical limitations of the kth equipment. The $\dot{E}_{D,k}^{EX,AV}$ is the irreversibility calculated in equipment k and it is avoidable by improving the efficiency of other remaining equipment. The $\dot{E}_{D,k}^{EX,UN}$ is the unavoidable part of the exogenous exergy destruction within kth equipment, which cannot be reduced due to the technical or economical limitations of the other equipment in the overall system.

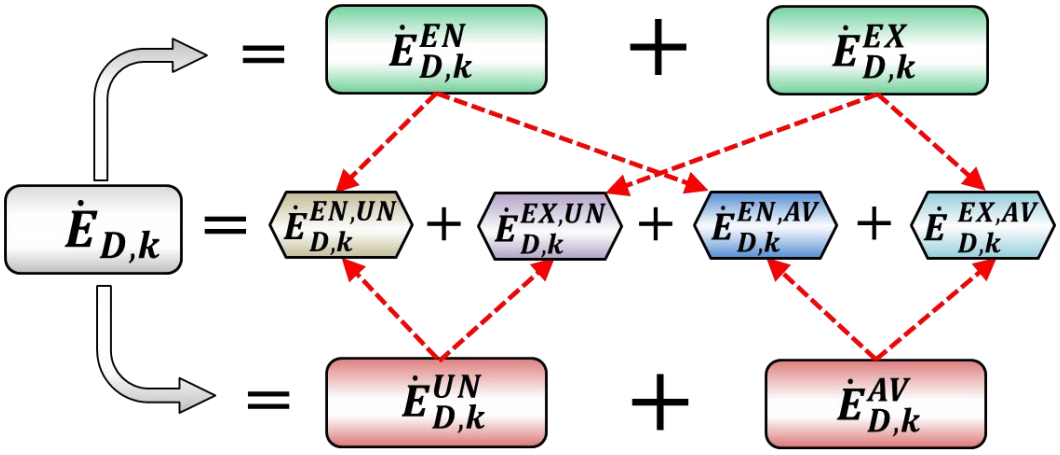

Fig. 3 Division of the exergy destruction within the k-th equipment.

Different parts of the total exergy destruction within the kth equipment are explicitly illustrated in Fig. 3. They can be calculated by Eqs. (16-19):

$$\dot{E}_{D,k}^{UN,EN} = \dot{E}_{D,k}^{UN}\left(\frac{\dot{E}_{D,k}^{EN}}{\dot{E}_{D,k}}\right) \tag{16}$$

$$\dot{E}_{D,k}^{UN,EX} = \dot{E}_{D,k}^{UN} - \dot{E}_{D,k}^{UN,EN} \tag{17}$$

$$\dot{E}_{D,k}^{AV,EN} = \dot{E}_{D,k}^{EN} - \dot{E}_{D,k}^{UN,EN} \tag{18}$$

$$\dot{E}_{D,k}^{AV,EX} = \dot{E}_{D,k}^{AV} - \dot{E}_{D,k}^{AV,EN} \tag{19}$$

3.3 The thermodynamic model of the single ORC system

Compared with some other heat sources (*e.g.*, solar energy) with constant temperature, the waste energy utilized in this study comes from several sensible heat sources. Therefore, the evaporator in the ORC must be divided into two parts involving a preheater and a vaporizer to consider the pinch point limitation. The detail models of basic ORC and ORC with a recuperator are illustrated in Fig. 4 (a) and (b), respectively. As for the basic single ORC, the inlet steam of the heat source (point 8) is applied to vaporize the working fluid, and then the remaining energy (point 9) is utilized to preheat the working fluid to the saturated liquid. The additional cooler is also added to condenser the stream to the suitable temperature as required in the existing process. However, if the temperature of the heat source outlet of the evaporator (point 10) meets the required value, adding an additional recuperator can effectively improve the energy recovery efficiency from the heat source. Thermodynamic performance indicators considered in this study are defined by Eq. (20) and (21).

The system efficiency of the ORC integrating with the heat source:

$$\eta_{ORC} = \frac{W_{net} - W_{pump}}{Q_{total}} \tag{20}$$

where W_{net} , W_{pump}, and Q_{total} represent output electrical power of the turbine, input electrical power of the pump, and total waste energy of the heat source, respectively.

The overall exergy destruction of the ORC integrating with the heat source:

$$E_{D,ORC} = \sum_{k} E_{D,k} \tag{21}$$

where $E_{D,k}$ is the exergy loss of each equipment k in the entire ORC system.

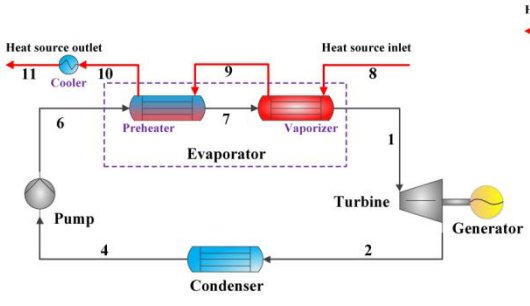

(a) Schematic diagram of detail single ORC model

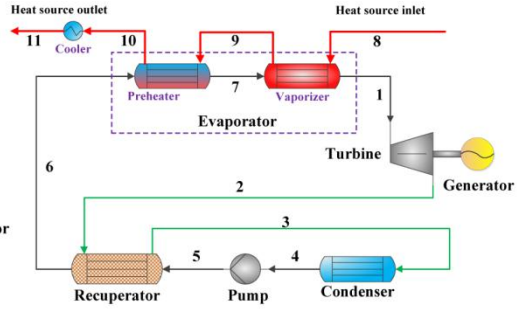

(b) Schematic diagram of detail single ORC model with recuperator

Fig. 4 (a) Schematic diagram of detailed single ORC system with a preheater; (b) Schematic diagram of detailed single ORC system with a preheater with an additional recuperator.

Some assumptions of the ORC system are made based on actual operation condition: (1) The overall system is operated in steady-state condition; (2) The working fluid at the outlet of preheater is considered as the saturated liquid (point 7), and temperature difference between the process stream at outlet of the vaporizer (point 9) and point 7 is set as 10 ℃; (3) The outlet temperature of cooling water is 30 ℃ [35] and the working fluid at condenser outlet (point 4) in the saturated state has a temperature of 10 ℃ higher than the incoming cooling water; (4) The isentropic efficiencies of the expander and the pump are respectively set to 85% and 70% [36]; (5) Pressure losses in the heat exchangers are neglected, however, the system is prepared to include pressure losses in the evaporator and condenser.

The selection of the working fluids is also a crucial factor in the ORC process [37]. The performance, system efficiency, and system stability of ORC process are determined by the working fluids with different thermo-physical properties [38]. The organic working fluids are divided into three types (including dry, wet and isentropic) based on their slope of saturation vapor line in the T-S diagram with positive, zero, and negative, respectively. Comparing with the dry and isentropic fluids, wet fluids have to be superheated in the evaporator because they may form droplet at the outlet of the turbine, and the presence of droplet may potentially decrease the isentropic efficiency of the turbine and damage the turbine [39, 40]. However, superheated working fluids will increase the heat exchanger area and the operation cost of the evaporator resulting from the reduction of the heat transfer coefficient between the vapor phase and the heat source. Additionally, it is found that superheating the dry working fluids will reduce the thermal efficiency of the ORC process and increase the exergy loss and irreversibility of the cycle [41]. Therefore, selecting the dry or isentropic organic fluids without superheating is the first priority.

The application range of the working fluids is also limited by their critical temperature and pressure. The ORC process adopting the organic substance with low critical temperature as working fluids may become a supercritical Rankine cycle, in

which the condenser requires more strict operation condition. For a subcritical ORC process without superheating, the temperature of saturated vapor at the out of the evaporator should be less than the critical temperature. It is found that using the working fluids with the critical temperature which approaches to the inlet temperature of the heat source can improve the energy efficiency of the ORC process [42, 43]. Other important thermo-physical properties (*e.g.,* the latent heat of vaporization, specific volume, environmental impacts, safety factor, and molecular weight) also should be considered in selecting the working fluids [44].

Considering all the above-mentioned factors, three organic substances including isopentane, N-pentane, and N-hexane are selected as the preselected working fluids in this study. The thermodynamic properties of three working fluids are obtained from Aspen Plus as listed in Table 1. The T-S diagram of selected working fluids is described in Fig. 5, showing that the three working fluids are all dry fluids.

Table 1 Properties of preselected working fluids.

Working fluid	Chemical formula	$T_{critical}$ (℃)	$P_{critical}$ (Mpa)	Global warming potential
isopentane	C_5H_{12}	187.2	3.396	very low
n-pentane	C_5H_{12}	196.6	3.370	very low
n-hexane	C_6H_{14}	234.7	3.034	very low

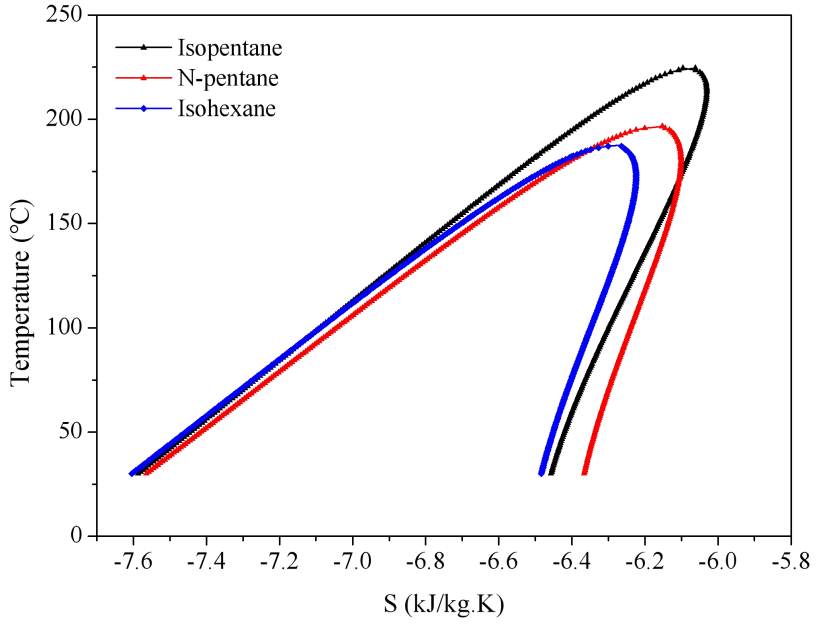

Fig. 5 T-S diagram of isopentane, N-pentane and N-hexane working fluids.

The pressure-temperature (P-T) diagram of three preselected working fluids is described in Fig. 6, which has significant guidance to determine the operation outlet pressure of the expander. In order to use the cooling water as medium in condenser, the lowest operation temperature of the condenser in ORC is assumed as 40 ℃. The operation pressure of the condenser should be higher than the saturated vapor pressure of the working fluid at 40 ℃ for avoiding vapor streams appearance at the inlet of pump.

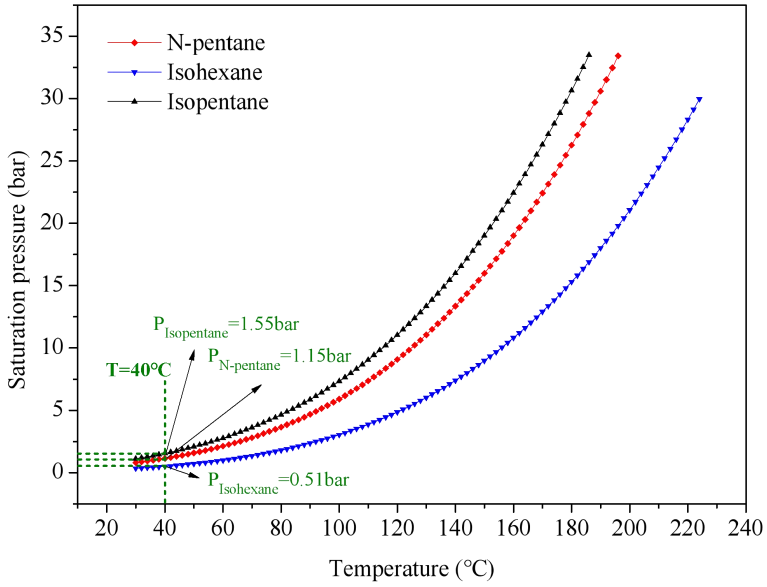

Fig. 6 P-T diagram of isopentane, N-pentane and N-hexane working fluids.

3.4 The economic assessment

In addition to the system efficiency and exergy loss of the overall ORC process, the economic analysis is employed to evaluate the proposed energy recovering schemes. Several objective functions such as net present value (NPV) [45], specific investment cost [46] and levelized cost of electricity [47] are usually selected. In this study, the annual net profit (ANP) is adopted as the objective function, which incorporates the total annualized cost (TAC) and the annual profit (AP) from the electrical power generation and it can be expressed as follow:

$$ANP = AP - TAC \tag{22}$$

The AP of the system is correlated with the annual operating hours (AOH), electricity price (Pr), and total electrical power output (W_{net}), and AP is calculated by Eq. (23) [48]:

$$AP = AOH \times Pr \times W_{net} \tag{23}$$

where the AOH and the Pr are 8000 h/year and 0.10 \$/(kW×h), respectively.

The TAC [49, 50] involving capital cost per year and operating cost can be calculated by Eq.24:

$$\text{TAC} = \text{annualized capital cost+operating cost} \tag{24}$$

The annualized capital cost (ACC) can be calculated by Eq.25:

$$\text{ACC} = \text{capital cost} \times \frac{i(1+i)^{\text{n}}}{(1+i)^{\text{n}}-1} = \text{captial cost} \times 0.021 \tag{25}$$

where i represents the fraction interest rate per year; n represents the number of years (i = 10% and n=25 years in this study [48]). Capital costs of the ORC system include heat exchangers costs, the condenser cost, the evaporator cost, the turbine cost, and the pump cost. In order to obtain the total investment cost, a cost correlation is used for each equipment of the system and is given in Table 2 [51, 52].

The mainly operating cost of the ORC system is due to the consumption of the cooling water in the condensers. The cost of the cold utility is considered as 20 \$/(kWyear).

Table 2 The cost of different types of equipments.

Equipment	Parameter variable	Cost [\$]
Expander	W_{net}(kW)	$430\times(W_{net}/4000)^{0.67}$
Heat exchangers	Heat exchange Area A (m^2)	$HX=7692.9\times A^{0.65}$
Pump	Electrical power	$900\times(W_{pump}/300)^{0.25}$
Working fluid	Mass M (kg)	20×M

4. Results and discussion

The Fischer-Tropsch syngas (FTS) process with DRM/SMR in parallel is taken as the existing process, and the compositions of FTS and captured CO_2 along with the energy balance of each equipment are compared with data from Baltrusaitis and Luyben [11, 12], as shown in Tables 3 and 4. The result shows that about 14930.00 kmol/h of H_2 and 7497.57 kmol/h of CO can be produced from the overall process.

The simulation results involving compositions of all the streams and the energy balance of every equipment of the existing process are aligned well with the published data [11, 12].

Table 3. Comparison of output streams between this study and published data.

STREAM	Gas to FT			Vaptured CO_2		
	This study	Baltrusaitis and Luyben [11]	Luyben [12]	This study	Baltrusaitis and Luyben [11]	Luyben [12]
T(℃)	116.3	115.0	125.0	90.0	90.0	90.0
P(bar)	30.0	30.0	33.0	10.0	9.8	9.9
Total flow (kmol/h)	22882.10	22924.90	22960.00	872.97	850.00	840.00
CH_4	271.21	286.00	245.00	0.00	0.00	0.00
H_2O	130.22	133.30	126.00	64.67	64.67	57.00
H_2	14930.90	14953.00	15005.00	21.30	0.00	0.00
CO_2	52.14	52.60	30.00	778.98	784.48	778.00
CO	7497.57	7500.00	7556.00	4.08	0.00	0.00
MEA	0.00	0.00	0.00	0.00	0.00	3.90

Table 4. Comparison of energy balance of the DRM/SMR process between this study and published data.

Equipment	Type	Energy or working cost(MW)		
		This study	Baltrusaitis and Luyben [11]	Luyben [12]
H-101	Heat Exchanger	5.999	5.610	6.040
H-102	Heat Exchanger	114.888	108.700	130.400
H-103	Heat Exchanger	117.000	26.370	117.000
SMR	Reactor	196.646	287.900	202.200
H-104	Heat Exchanger	9.311	100.100	9.100
H-105	Heat Exchanger	16.045	41.280	16.000
H-106	Heat Exchanger	94.886	94.860	96.300
H-107	Heat Exchanger	34.680	44.830	34.700
H-108	Heat Exchanger	39.200	37.600	47.200
H-109	Heat Exchanger	78.090	70.500	80.600
H-110	Heat Exchanger	30.560	31.400	31.600
C-101	Compressor	4.480	4.470	4.470
DRM	Reactor	186.086	188.900	200.500
H-111	Heat Exchanger	74.110	74.130	66.200
H-112	Heat Exchanger	14.008	13.980	22.000

C-102	Compressor	12.231	12.230	13.400
H-113	Heat Exchanger	12.257	12.280	12.200
C-103	Compressor	12.416	12.390	13.600

4.1 The result of conventional exergy analysis

The detailed computing results of existing processes based on CEA are presented in Table 5. The total exergy input and output of the overall process are 1837.58 MW and 1732.22 MW, respectively. Consequently, the exergy efficiency of the overall process is 94.27%. According to Table 5, it is apparent that the maximum value of exergy destruction (22.51 MW) occurs in the heat exchanger (H-106) resulting from the outlet gas from SMR is cooled by the cooling water. The 14.85% and 9.19% of the total exergy destruction are destroyed in SMR and DRM because both the two reactors are operated at high temperatures. The condenser and reboiler in the stripper (T-102) have relatively large exergy destructions, and their exergy efficiencies are 92.62% and 52.31%, respectively. As for other equipments, the temperature drop is the main reason of the exergy destruction in the heat exchangers, and small exergy destruction is caused by compressors and the pumps due to the irreversibility.

Table 5. Computing results of the DRM/SMR processes based on CEA.

Equipment	$\dot{E}_{D,k}$ (MW)	$\dot{E}_{F,k}$ (MW)	$\dot{E}_{P,k}$ (MW)	ε_k (%)	y_k (%)	y_k^* (%)
H-101	1.0519	740.1080	739.0560	99.86	0.06	0.95
P-101	0.0240	28.0667	28.0427	99.91	0.00	0.02
H-102	3.8536	77.9353	74.0817	95.06	0.21	3.48
H-103	4.8840	1806.1100	1801.2300	99.73	0.27	4.41
SMR	16.4466	1028.3949	1011.9483	**98.40**	**0.90**	**14.85**
H-104	0.7260	919.3800	918.6540	99.92	0.04	0.66
H-105	2.0553	913.6530	911.5980	99.78	0.11	1.86
H-106	**22.5060**	908.2220	885.7160	**97.52**	**1.22**	**20.32**
T-101	0.5814	871.7734	871.1920	99.93	0.03	0.52
H-107	2.0372	1735.8000	1733.7600	99.88	0.11	1.84
H-108	7.4619	862.7410	855.2790	99.14	0.41	6.74
T-102	9.3787	950.5673	941.1885	99.01	0.51	8.47
H-109	5.8143	78.7624	72.9481	92.62	0.32	5.25
H-110	6.8004	14.2591	7.4587	52.31	0.37	6.45
C-101	0.6799	19.5243	18.8445	96.52	0.04	0.61
DRM	10.1770	838.7773	828.6003	**98.79**	**0.55**	**9.19**

H-111	1.4910	1472.6700	1471.1800	99.90	0.08	1.35
H-112	3.1136	775.3160	772.2020	99.60	0.17	2.81
C-102	1.8736	784.4160	782.5420	99.76	0.10	1.69
H-113	2.4990	782.1080	779.6090	99.68	0.14	2.26
C-103	1.8981	792.0250	790.1270	99.76	0.10	1.71
TOTAL	105.3537	1837.5795	1732.2258	94.27	5.72	100.00

ε_k, exergy efficiency of k-th equipment;

y_k, exergy destruction ratio of k-th equipment;

y_k^*, the ratio of the exergy destruction within the kth equipment to the total exergy destruction of the system.

4.2 Advanced exergy analysis

The advanced exergy analysis (AEA) using the combined splitting of unavoidable and avoidable as well as endogenous and exogenous exergy destruction is taken to analysis the overall process. The computing results of each equipment based on the AEA are summarized in Table 6.

4.2.1 Endogenous/Exogenous exergy destruction

The analysis of equipment interaction is quantified by splitting exergy destruction within the k-th equipment into endogenous and exogenous parts (the first and second column in Table 6). The exogenous exergy destruction caused by the exchanger H-103 is more than the other equipments because the operation condition of the H-103 is depended on the SMR. It also can be observed from Fig. 7 that the 92.90% exergy destruction in overall process is endogenous. The high endogenous exergy destruction indicates that the interactions of each equipment do not significantly increase the thermodynamic irreversibility of the overall process. Therefore, it is necessary to improve the operation conditions of the equipment within the high endogenous exergy destruction (*e.g.*, Exchanger H-106 and H-110) for the aim of energy saving.

Table 6. Results of advanced exergetic analysis of DRM/SMR processes.

Equipment k	Exergy destruction (MW)							
	$\dot{E}_{D,k}^{EN}$	$\dot{E}_{D,k}^{EX}$	$\dot{E}_{D,k}^{UN}$	$\dot{E}_{D,k}^{AV}$	$\dot{E}_{D,k}^{UN,EN}$	$\dot{E}_{D,k}^{AV,EN}$	$\dot{E}_{D,k}^{UN,EX}$	$\dot{E}_{D,k}^{AV,EX}$
H-101	1.0519	0.0000	0.7290	0.3229	0.7290	0.3229	0.0000	0.0000
P-101	0.0240	0.0000	0.0035	0.0205	0.0035	0.0205	0.0000	0.0000
H-102	3.8536	0.0000	1.4580	2.3956	1.4580	2.3956	0.0000	0.0000

H-103	2.3625	2.5215	1.7390	3.1450	0.8397	1.5228	0.8993	1.6222
SMR	14.160	2.2857	16.363	0.0836	14.088	0.0720	2.2741	0.0116
H-104	0.6886	0.0374	0.0970	0.6290	0.0920	0.5966	0.0050	0.0324
H-105	1.9644	0.0908	0.8480	1.2073	0.8105	1.1539	0.0375	0.0534
H-106	22.506	0.3661	7.1650	15.341	7.0484	15.091	0.1166	0.2496
T-101	0.5814	0.0000	0.5814	0.0000	0.5814	0.0000	0.0000	0.0000
H-107	1.0237	1.0136	1.9616	0.0757	0.9856	0.0381	0.9760	0.0376
H-108	7.4620	0.0000	1.3507	6.1113	1.3507	6.1113	0.0000	0.0000
T-102	9.3787	0.0000	9.3787	0.0000	9.3787	0.0000	0.0000	0.0000
H-109	5.8143	0.0000	0.7730	5.0413	0.7730	5.0413	0.0000	0.0000
H-110	6.8004	0.0000	2.1496	4.6508	2.1496	4.6508	0.0000	0.0000
C-101	0.6799	0.0000	0.2588	0.4211	0.2588	0.4211	0.0000	0.0000
DRM	9.7999	0.4772	10.207	0.0697	9.7334	0.0665	0.4739	0.0032
H-111	0.8008	0.6902	0.7700	0.7210	0.4133	0.3874	0.3567	0.3336
H-112	3.1136	0.0000	0.1150	2.9986	0.1150	2.9986	0.0000	0.0000
C-102	1.8666	0.0070	0.7124	1.1612	0.7103	1.1563	0.0021	0.0049
H-113	2.4990	0.0000	0.6400	1.8590	0.6400	1.8590	0.0000	0.0000
C-103	1.8981	0.0000	0.7226	1.1754	0.7226	1.1754	0.0000	0.0000
TOTAL	97.964	7.4896	58.023	47.430	52.882	45.081	5.1411	2.3485

4.2.2 Unavoidable and avoidable exergy destruction

The exergy destruction of each equipment can be reduced by improving the operation condition once technical and economic limitations are satisfied. Hence, it is necessary to split the exergy destruction within the overall process and every equipment into unavoidable and avoidable parts. In this work, the unavoidable conditions of different kinds of equipments are listed in the Table 7, and the results are summarized in the third and fourth column of Table 6 and described in Fig. 7. It can be found that the existing process has great potential in energy-saving because 44.98% exergy destruction of the overall process can be avoidable. The largest values of avoidable exergy 15.34 MW are destructed in the heat exchanger H-106, followed by H108, H-110, H-109, and H-112.

Table 7. Condition assumptions of the unavoidable exergy destruction.

Equipment	Unavoidable condition
Compressor	Isentropic efficiency = 90%
Heat changer	Minimum temperature approach = 5.0 ℃
Reactor	Gibbs reactor with constant reactor
Pump	Isentropic efficiency = 90%
Distillation column without reboiler and Condenser	No Improvement Potential

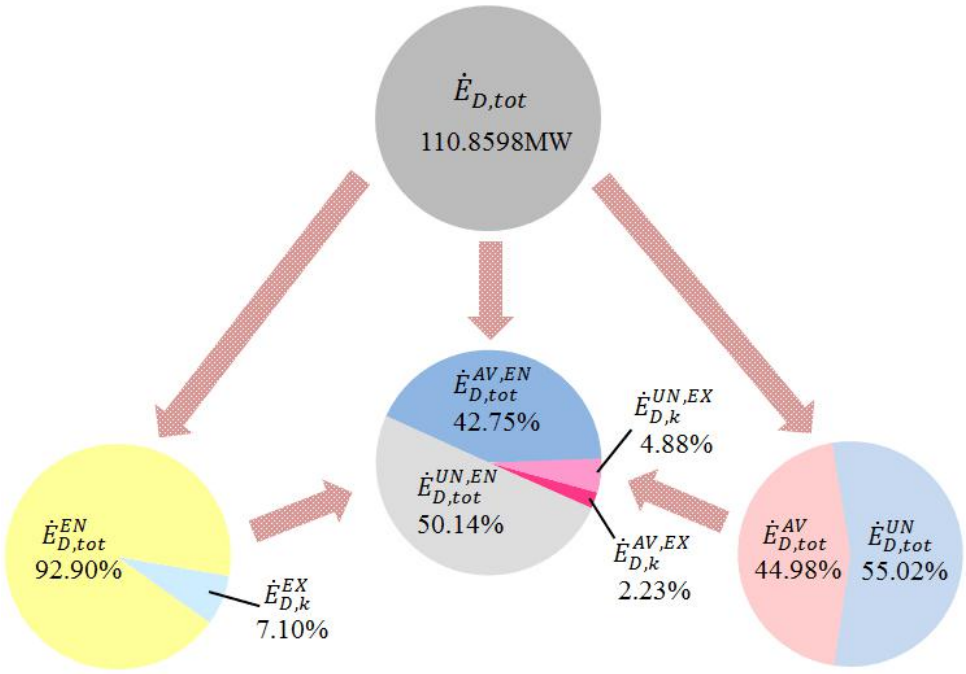

Fig. 7 Division of total exergy destruction of entire SMR / DMR process.

4.2.3 Combined exergy destruction analysis based on four divisions

The total exergy destruction within equipment k-th by using the combined splitting of unavoidable and avoidable as well as endogenous and exogenous exergy destruction as shown in Table 6. It is necessary to focus on the avoidable endogenous exergy destruction which indicates the independent improvement potential of each equipment. As is evident in Fig. 7, avoidable endogenous exergy destruction 42.75% of the overall process is higher than the avoidable exogenous exergy destruction 4.88%. The largest avoidable endogenous exergy destruction is taken in the heat exchanger H-106, followed by H-108, H-109. And avoidable endogenous exergy destructions of H-108 and H-109 occupy the most of their total exergy destruction, which means that it is difficult to further utilize the energy from two heat exchangers. The heat exchangers H-112 and H-113 have smaller exergy destruction while the avoidable endogenous exergy destructions of two equipments are relatively high. The endogenous exergy destruction of the other equipments in the system is difficult to be reduced due to the technical and economic limitations. Consequently, it is important to recovery the energy from the heat exchangers H-106, H-110, H-112 and H-113 because the condenser water with low exergy value is selected as the cooling

medium in four heat exchangers.

4.3 The application and optimization of the ORC system

A significant waste heat in some heat exchangers involving H-106, H-109, H-112 and H-113 in the reference process can be utilized based on the AEA. The inlet temperatures of four sensible heat sources are all approach to 200 ℃ as illustrated in Fig. 1. To recover the energy from each sensible heat source, the ORC system without or with a recuperator are applied for electrical power generation. For improving the performance of the ORC system, operation parameters including working fluid and the inlet temperature of the turbine in every single ORC should be optimized with both system efficiency and total exergy destruction of ORC working as objective functions.

4.3.1 The optimization of the ORC with the H-106 as waste heat source

The single ORC system with the H-106 as waste heat source is analyzed to improve the efficiency of the energy utilization. As a sensible heat source, the H-106 waste heat source though has the fixed inlet temperature and heat duty. Therefore, effects of the turbine inlet temperature and working fluids on the exergy loss and thermal efficiency of the ORC system with a recuperator are studied as illustrated in the Fig. 8. The optimal evaporating temperatures of three working fluids and the temperature-thermal load diagram of the H-106 are described in Fig. 9. It is found that the optimal turbine inlet temperatures with isopentane, n-pentane and isohexane as working are 140.3 ℃, 145.2 ℃ and 134.3 ℃, respectively. Compared to other two organic mediums, selecting the n-pentane as the working fluids has highest system thermal efficiency (15.75%) and lowest exergy loss (8.04 MW).

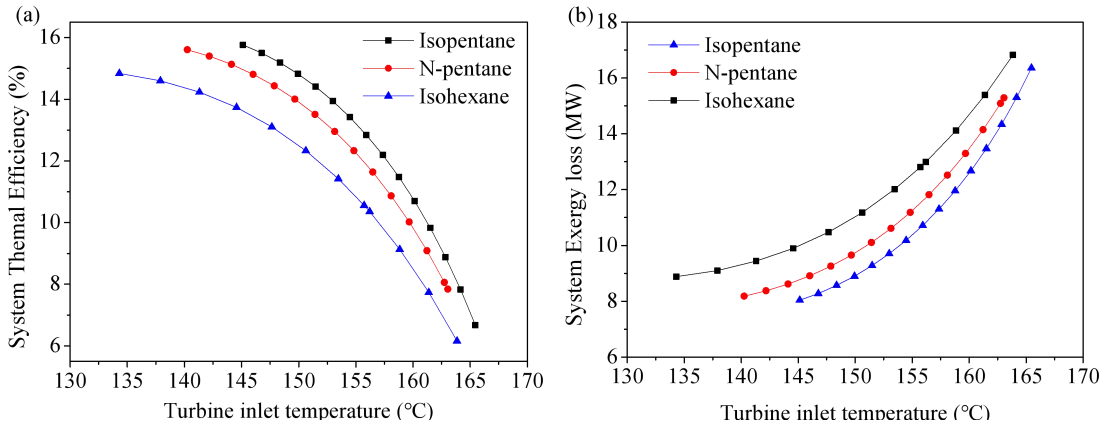

Fig. 8 The H-106 integrating with the ORC system with a recuperator (a) The system efficiency depending on the turbine inlet temperature (b) The system exergy loss depending on the turbine inlet temperature.

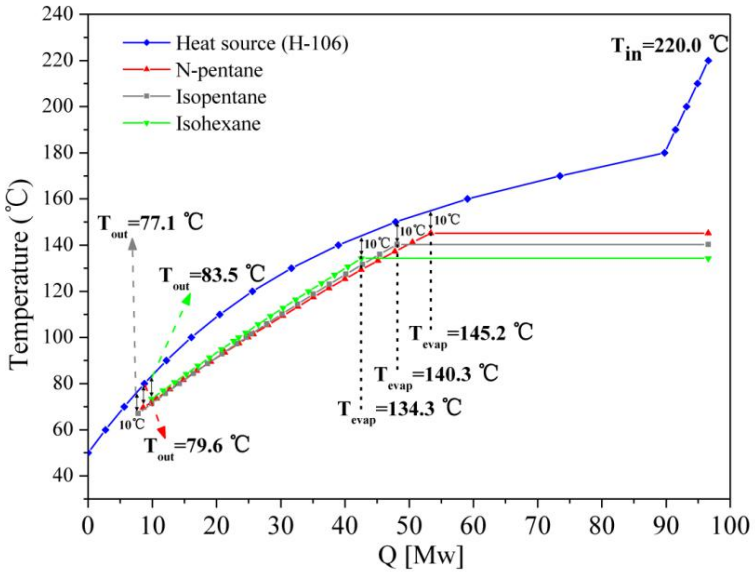

Fig. 9 T-Q diagram of the H-106 integrating with the ORC with a recuperator by using three preselected working fluids at optimal operation condition.

4.3.2 The optimization of the ORC with the H-110 as waste heat source

The single ORC system with a recuperator for recovering the waste energy in H-110 is optimal designed based on theoretical analysis in the Section 4.3.1. The effects of the turbine inlet temperature on system thermal efficiency and exergy efficiency are illustrated in Fig. 10. The temperature-thermal load of the H-110 and optimal operation conditions of three working fluids are illustrated in Fig. 11. The process stream of the H-110 is condensed from 167.8 ℃ to 90.0 ℃, meanwhile, the working fluids is heated from 40 ℃ to their respective optimal evaporating temperature. The optimal evaporating temperatures with isopentane, n-pentane, and isohexane as working fluids are 147.6 ℃, 145.9 ℃ and 142.0℃, respectively. The highest system efficiency and lowest system exergy loss are 17.60% and 2.62 MW with the n-pentane as working fluid.

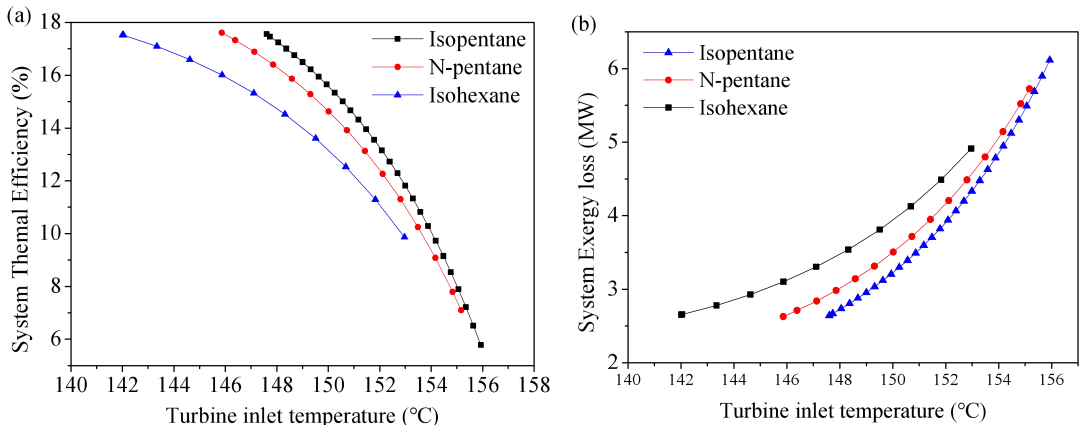

Fig. 10 The H-110 integrating with the ORC system with a recuperator (a) The system efficiency depending on the turbine inlet temperature (b) The system exergy loss depending on the turbine inlet temperature.

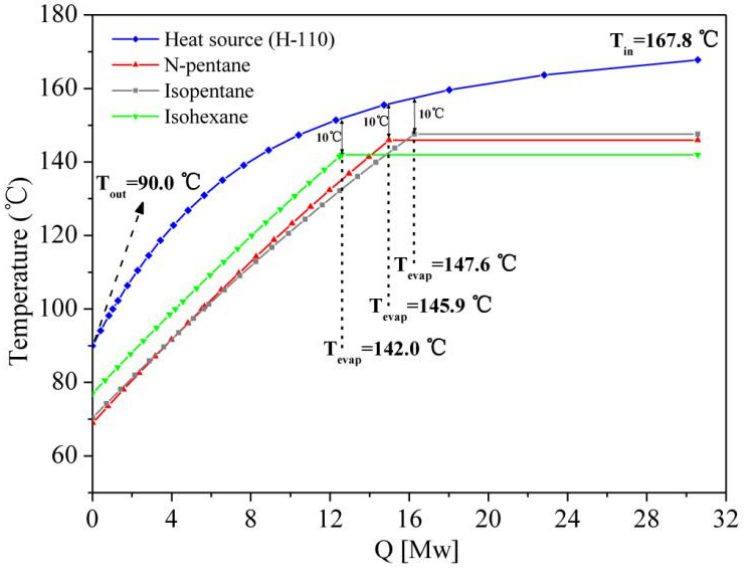

Fig. 11 T-Q diagram of the H-110 integrating with the ORC with a recuperator by using three preselected working fluids at optimal operation condition.

4.3.3 The optimization of the ORC with the H-112 as waste heat source

The single ORC system is also optimal designed to improve the thermodynamic performance of the energy utilization process. Fig. 12 shows the effects of the turbine inlet temperature and working fluids on the exergy loss and thermal efficiency ORC system without recuperator. As illustrated in Fig. 12 (a), when the turbine inlet temperature is increased, the system efficiency of the ORC with three preselected working fluids is firstly raised up and then decreased while the overall exergy loss is

firstly decreased and then increased. The optimal evaporating temperatures of three working fluids and the temperature-thermal load diagram of the H-112 are described in Fig. 13. It is found that the ORC using isopentane as the working fluids has highest system efficiency 14.46% and lowest exergy loss 1.33 MW. As shown in Fig. 13, the stream temperature at the outlet of the preheater is higher than the required condensing temperature (50 ℃). As such, an additional condenser is required to be added to cool the process stream instead of introducing a recuperator.

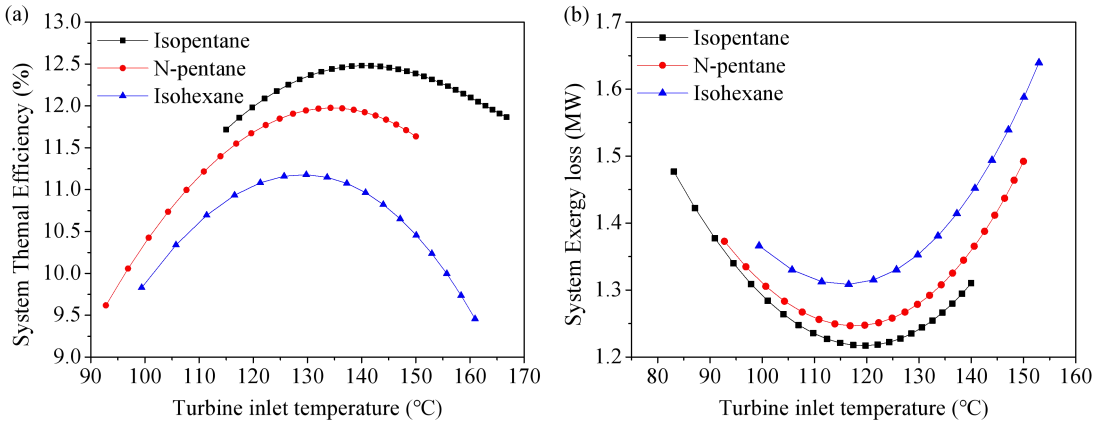

Fig. 12 The H-112 integrating with the basic ORC system: (a) The system efficiency depending on the turbine inlet temperature; (b) The system exergy loss depending on the turbine inlet temperature.

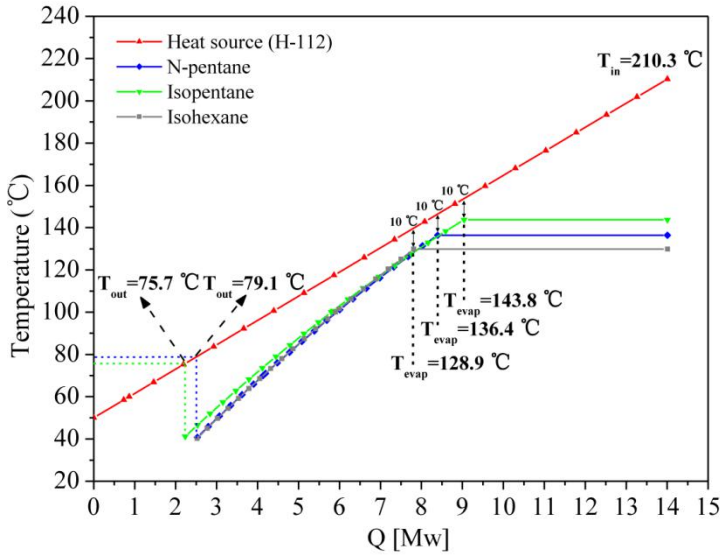

Fig. 13 T-Q diagram of the H-112 integrating with the basic ORC with three preselected working fluids at optimal operation condition.

4.3.4 The optimization of the ORC with the H-113 as waste heat source

Fig. 14 demonstrates effects of the turbine inlet temperature and working fluids on the exergy loss and thermal efficiency of ORC system without a recuperator. Compared to the n-pentane and isohexane, the ORC with the isopentane as the working fluid has the great performance of energy utilization. The optimal system efficiency and exergy loss are respective 10.23% and 1.21 MW when the turbine inlet temperature of the isopentane is operated at 120.7 ℃. The temperature-thermal load diagram of the H-113 and optimal evaporating temperatures of three working fluids are described in Fig. 15. The temperature of the heat source is condensed from 189.9 ℃ to 80.1 ℃ with the isopentane as the working fluid. Therefore, it has no significance to introduce a recuperator to improve the ORC since the temperature of the process stream at the outlet of the preheater is higher than the required temperature.

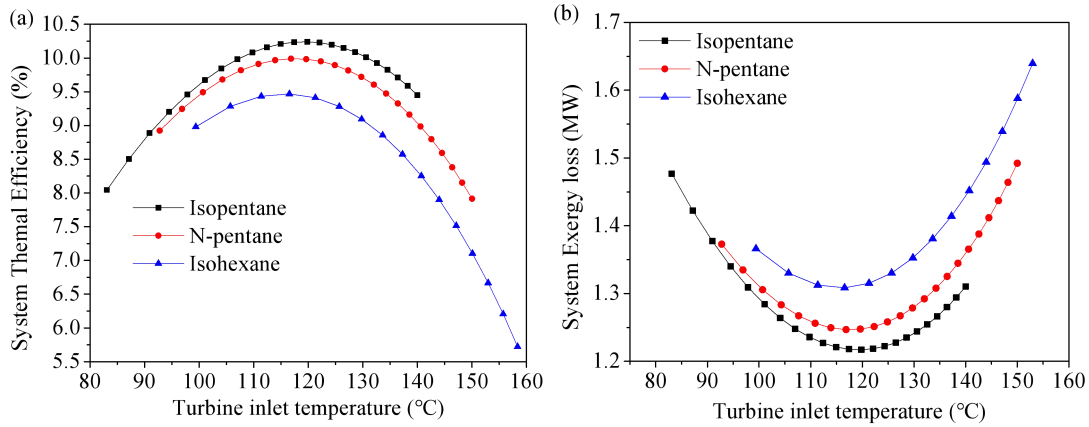

Fig. 14 The H-113 integrating with the basic ORC system: (a) The system efficiency depending on the turbine inlet temperature; (b) The system exergy loss depending on the turbine inlet temperature.

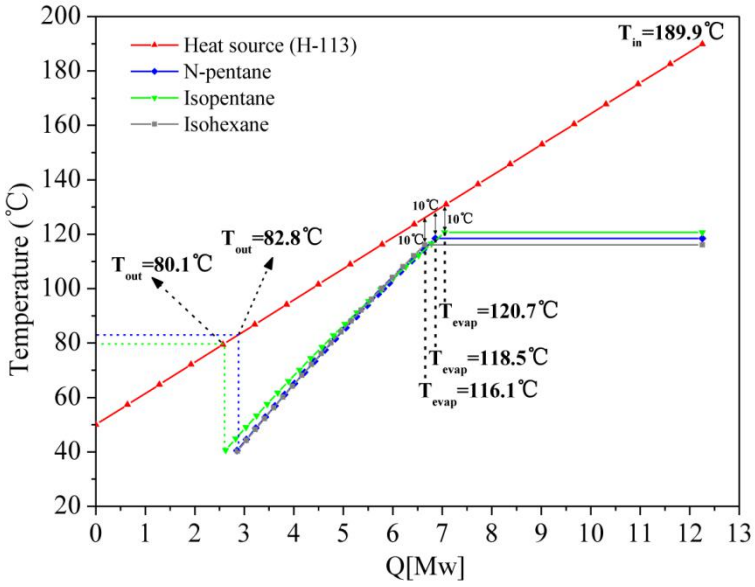

Fig. 15 T-Q diagram of H-113 integrating with the basic ORC with three preselected working fluids at optimal operation condition.

4.4 Combined ORC systems with different schemes

The four optimal single ORC systems integrating each heat source are illustrated in Fig. 16 based on the Section 4.3. The isopentane is selected as the working fluid while the waste heat coming from H-106, H-112, and H-113. Meanwhile, using the n-pentane as the working fluid can efficiently utilize the energy from H-110 for electrical power generation. The optimal evaporator temperatures are very close (*i.e.*, 145.2℃, 147.6℃ and 143.8℃ respectively) when the isopentane is adopted as the working fluid in three single ORCs. As a consequence, in order to reduce the equipment investment, combined ORC systems with two turbines and a dual-pressure ORC system are proposed in Fig. 17 and Fig. 18, respectively.

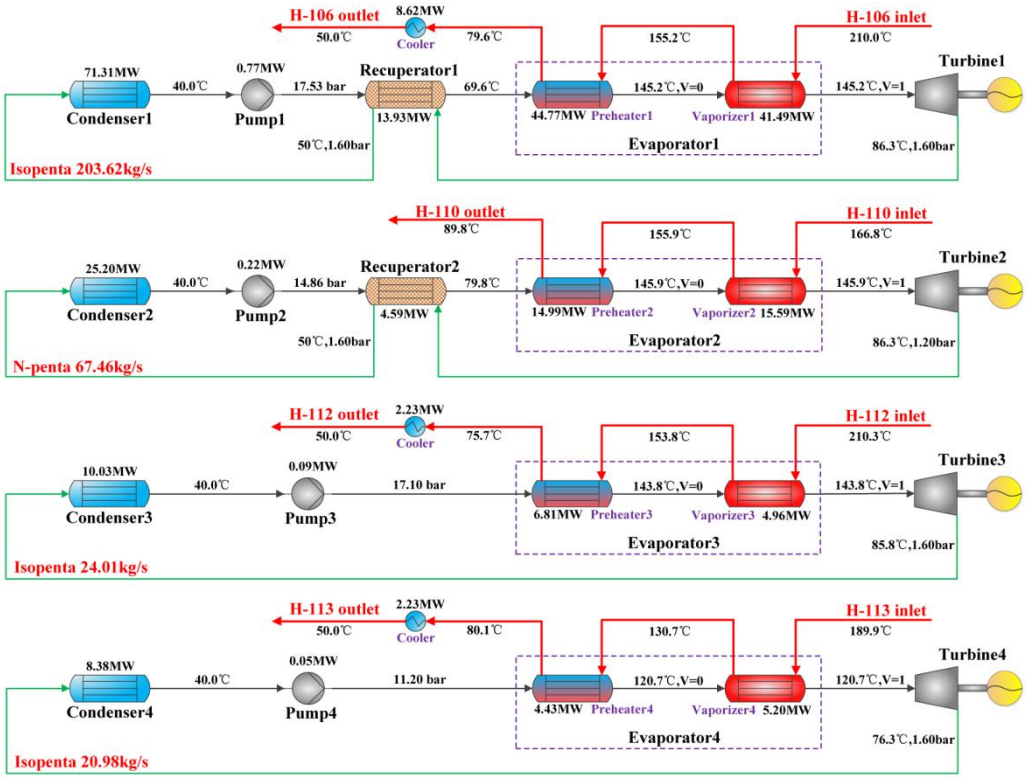

Fig. 16 Four optimal single ORC systems integrating with each heat source in the existing process.

According to Fig. 17, it is apparent that three ORC systems using H-106, H-110 and H-112 as the heat sources are combined with one turbine for electric generation. In order to reduce the exergy loss in the turbine 1, the evaporation temperatures of evaporator 1, evaporator 2 and evaporator 3 are equal with 145.2 ℃. The stream at the out let of the turbine 1 with 86.3 ℃, 1.6 bar is splited and then used to preheat the condensered working fluid in the recuperator 1 and the recuperator 2. The single ORC system is applied to recovery the waste energy in H-113 with low inlet pressure of turbine 11.2 bar .

Based on the combined ORC systems, a dual-pressure ORC system is proposed to improve the system thermal efficiency and exergy efficiency as illustrated in Fig. 18. The mixed saturated stream of the isopentane at 17.53 bar, 145.2 ℃ is expanded to 11.2 bar, 130.0 ℃ in turbine 1. Then, it combined with the saturated steam 11.2 bar, 120.0 ℃ at the outlet of the evaporator 4 are further expanded. The expanded vapor 1.6 bar, 85.5 ℃ at the outlet of the turbine 2 are divided into two parts for preheating the condensed working fluid in the recuperator 1 and the recuperator 2.

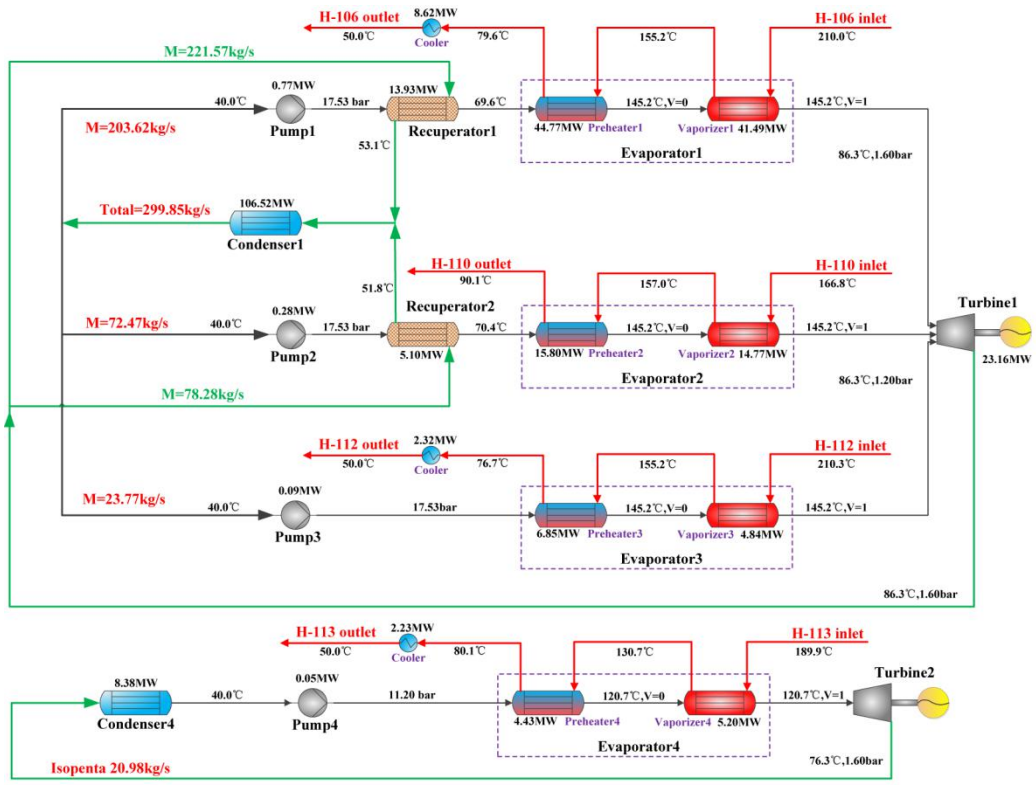

Fig. 17 System layouts of the combined ORC systems with two independent turbines.

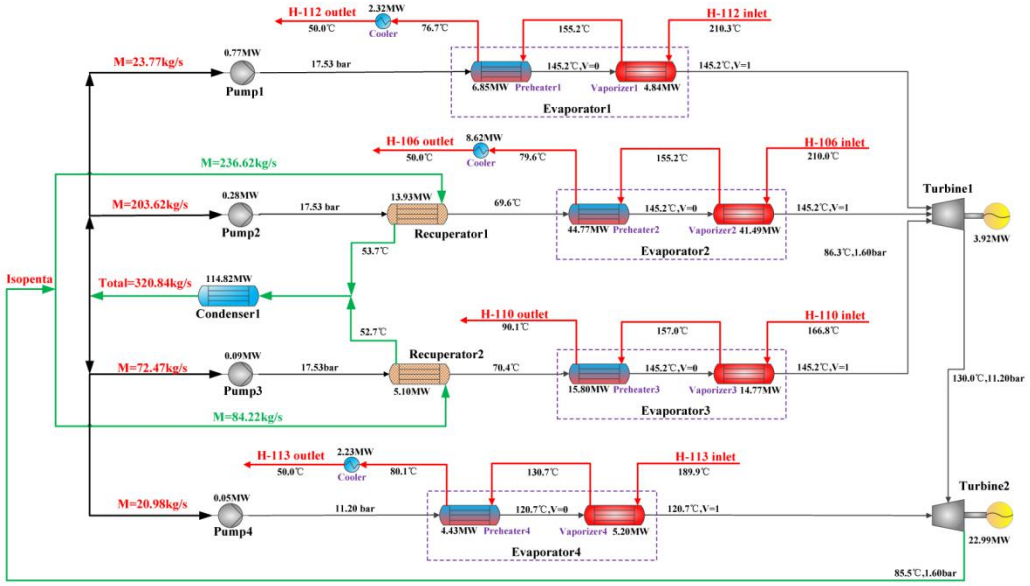

Fig. 18 System layouts of the optimal dual-pressure ORC system for electrical power generation.

The efficiency and economic comparison among the three proposed ORC schemes are summarized in Table 8. The dual-pressure ORC system has the best

performance with highest thermal efficiency 15.39% and annual net profit (ANP) 1.55 E+07 $/year. The simple payback period is calculated to be 4.60 years. Compared to the total exergy loss of the existing process, the exergy loss of the ORC systems is reduced from 34.92 MW to 13.21 MW. Around 88.21% of avoidable endogenous exergy destructions 21.71 MW in four heat exchangers are decreased on the basis of the proposed dual-pressure ORC system.

Table 8
The thermodynamic comparison and economic evaluation of three proposed ORC schemes

Three schemes		Four single ORCs	The combined ORCs	The dual-pressure ORCs
Net power output(MW)		24.45	24.46	24.54
Thermal efficiency (%)		15.37	15.34	15.39
System exergy loss(MW)		13.22	13.30	13.21
TAC(10^6$/year)	ACC	0.60	0.54	0.55
	OC	7.77	7.88	7.88
AP(10^6$/year)		23.88	23.87	23.95
ANP(10^6$/year)		15.51	15.45	15.52
Payback period		4.78	4.61	4.60

5. Conclusions

The thermodynamic performance of Fischer-Tropsch syngas production process is evaluated by combining the conventional and advance exergy analysis approaches in this study. Based on the theoretical exergy analysis, optimal schema with dual-pressure ORC system is designed for further energy recovering. The irreversibility of each equipment and the exergy loss distribution analysis of overall process are studied based on the CEA. The AEA is adopted to evaluate overall process, and the computing results indicate the energy saving potential of each equipment and thermodynamic interactions among equipments. The ORC with or without recuperators are applied to recovery the waste heat from existing process with the guidance of the exergy analysis framework.

It is found that ORCs have great performance by adopting the isopentane as the

working fluid. The inlet temperature of evaporator and the outlet pressure of turbine are optimized by using the system thermal efficiency and total exergy destruction of the ORC as the objective functions. The dual-pressure ORC system has the best performance with highest system thermal efficiency 15.39% and greatest annual net profit (ANP) 1.55 E+07 $/year. Considering total exergy loss of waste heat sources in the reference process, the exergy loss of the system integrating with the dual-pressure ORC scheme is reduced from 34.92 MW to 13.21 MW, and 88.21% of avoidable endogenous exergy destructions 21.71 MW in waste heat sources are decreased.

Acknowledgment

We acknowledge the financial support provided by the National Natural Science Foundation of China (Nos. 21878028, 21606026); the Chongqing Social livelihood Technological Innovation and Application Demonstration (No. CSTC2018JSCX-MSYBXX0336); the Fundamental Research Funds for the Central Universities (No. 2019CDQYHG021); the Chongqing Research Program of Basic Research and Frontier Technology (No. CSTC2016JCYJA0474); the Chongqing Innovation Support Program for Returned Overseas Chinese Scholars (No. CX2018048); the Hundred Talents Program at Chongqing University.

References

[1] Panahi M, Yasari E, Rafiee A. Multi-objective optimization of a gas-to-liquids (GTL) process with staged Fischer-Tropsch reactor. Energy Convers Manage 2018;163:239-49.

[2] Selvatico D, Lanzini A, Santarelli M. Low Temperature Fischer-Tropsch fuels from syngas: Kinetic modeling and process simulation of different plant configurations. Fuel 2016;186:544-60.

[3] Rafati M, Wang LJ, Dayton DC, Schimmel K, Kabadi V, Shahbazi A. Techno-economic analysis of production of Fischer-Tropsch liquids via biomass gasification: The effects of Fischer-Tropsch catalysts and natural gas co-feeding. Energy Convers Manage 2017;133:153-66

[4] Yang Y, Liu J, Shen WF, Li J, Chien IL. High-efficiency utilization of CO_2 in the methanol production by a novel parallel-series combing steam and dry

methane reforming. Energy 2018;158:820-9.

[5] Hernandez B, Martin M. Optimization for biogas to chemicals via tri-reforming. Analysis of Fischer-Tropsch fuels from biogas. Energy Convers Manage 2018;174:998-1013.

[6] Rahbari A, Shirazi A, Venkataraman MB, Pye J. A solar fuel plant via supercritical water gasification integrated with Fischer-Tropsch synthesis: Steady-state modelling and techno-economic assessment. Energy Convers Manage 2019;184:636-648.

[7] Panahi M, Rafiee A, Skogestad S, Hillestad M. A Natural Gas to Liquids Process Model for Optimal Operation. Ind Eng Chem Res 2012;51:425-433.

[8] Tabrizi FF, Mousavi SAHS, Atashi H. Thermodynamic analysis of steam reforming of methane with statistical approaches. Energy Convers Manage 2015;103:1065-77.

[9] Shahhosseini HR, Farsi M, Eini S. Multi-objective optimization of industrial membrane SMR to produce syngas for Fischer-Tropsch production using NSGA-II and decision makings. J Nat Gas Sci Eng 2016;32:222-38.

[10] Ryi SK, Lee SW, Park JW, Oh DK, Park JS, Kim S S. Combined steam and CO_2 reforming of methane using catalytic nickel membrane for gas to liquid (GTL) process. Catal Today 2014;236:49-56.

[11] Baltrusaitis J, Luyben WL. Methane Conversion to Syngas for Gas-to-Liquids (GTL): Is Sustainable CO_2 Reuse *via* Dry Methane Reforming (DMR) Cost Competitive with SMR and ATR Processes? Sustainable Chem Eng 2015;3:2100-11.

[12] Luyben WL. Control of parallel dry methane and steam methane reforming processes for Fischer-Tropsch syngas. J Process Contr 2016;39:77-87.

[13] Rezaei E, Dzuryk S. Techno-economic comparison of reverse water gas shift reaction to steam and dry methane reforming reactions for syngas production. Chem Eng Res Des 2019;144:354-69.

[14] Jain V, Sachdeva G, Kachhwaha SS. Comparative performance study and advanced exergy analysis of novel vapor compression-absorption integrated refrigeration system. Energy Convers Manage 2018;172:81-97.

[15] Vatani A, Mehrpooy M, Palizdar A. Advanced exergetic analysis of five natural gas liquefaction processes. Energ Convers Manage 2014;78:720-37.

[16] Yang QC, Qian Y, Kraslawski A, Zhou HR, Yang SY. AEA of an oil shale retorting process. Appl Energy 2016;165:405-15.

[17] Mehrpooya M, Lazemzade R, Sadaghiani MS, Parishani Hossein. Energy and AEA of an existing hydrocarbon recovery process. Energ Convers Manage 2016;123:523-34.

[18] Penkuhn M, Tsatsaronis G. Comparison of different ammonia synthesis loop configurations with the aid of AEA. Energy 2017;137:854-64.

[19] Rashwan SS, Dincera I, Mohany A. Analysis and assessment of cascaded closed loop type organic Rankine cycle. Energ Convers Manage 2019;184:416-26.

[20] Baldassoa E, Andreasena JG, Mondejara ME, Larsenb U, Haglind F. Technical and economic feasibility of organic Rankine cycle-based waste heat recovery systems on feeder ships: Impact of nitrogen oxides emission abatement technologies. Energ Convers Manage 2019;183:577-89.

[21] Pierobon L, Nguyen TV, Larsen U, Haglind F, Elmegaard B. Multi-objective optimization of organic Rankine cycles for waste heat recovery: Application in an offshore platform. Energy 2013;58:538-49.

[22] Li L, Ge YT, Luo X, Tassou SA. Thermodynamic analysis and comparison between CO_2 transcritical power cycles and R245fa organic Rankine cycles for low grade heat to power energy conversion. Appl Therm Eng 2016;106:1290-99.

[23] Yu HS, Eason John, Biegler T L. Feng X. Simultaneous heat integration and techno-economic optimization of Organic Rankine Cycle (ORC) for multiple waste heat stream recovery. Energy 2015;90:36-46.

[24] Yu HS, Feng X, Wang YF. A new pinch based method for simultaneous selection of working fluid and operating conditions in an ORC (Organic Rankine Cycle) recovering waste heat. Energy 2017;119:322-33.

[25] Song CF, Liu QL, Ji N, Deng S, Zhao J, Kitamura Y. Natural gas purification by heat pump assisted MEA absorption process. Appl Energy 2017;204:353-61.

[26] Rahbar K, Mahmoud S, Al-Dadah RK, Moazami N, Mirhadizadeh SA. Review

of organic Rankine cycle for small-scale applications. Energ Convers Manage 2017;134:135-55.

[27] Li XX, Zhou HR, Wang YJ, Qian Y, Yang SY. Thermoeconomic analysis of oil shale retorting processes with gas or solid heat carrier. Energy 2015;87:605-14.

[28] Szargut J, Morris DR, Steward FR. Exergy analysis of thermal, chemical and metallurgical processes. New York:Hemisphere Publishing Co; 1988.

[29] Galindo J, Ruiz S, Dolz V, Royo-Pascual L. Advanced exergy analysis for a bottoming organic rankine cycle coupled to an internal combustion engine. Energ Convers Manage 2016;126:217-27.

[30] Mehrpooya M, Ansarinasab H, Sharifzadeh MMM, Rosen MA. Conventional and advanced exergoeconomic assessments of a new air separation unit integrated with a carbon dioxide electrical power cycle and a liquefied natural gas regasification unit. Energ Convers Manage 2018;163:151-68.

[31] Zhang XF, Li HQ, Liu LF, Bai CY, Wang S, Song QB, Zeng J, Liu XB, Zhang GQ. Exergetic and exergoeconomic assessment of a novel CHP system integrating biomass partial gasification with ground source heat pump. Energ Convers Manage 2018;156:666-79.

[32] Palizdar A, Ramezani T, Nargessi Z, AmirAfshar S, Abbasi M, Vatani A. Thermodynamic evaluation of three mini-scale nitrogen single expansion processes for liquefaction of natural gas using advanced exergy analysis. Energ Convers Manage 2017;150:637-50.

[33] Kelly S, Tsatsaronis G, Morosuk T. Advanced exergetic analysis: Approaches for splitting the exergy destruction into endogenous and exogenous parts. Energy 2009;34: 384-391.

[34] Chen JY, Zhu KD, Huang YS, ChenY, Luo XL. Evaluation of the ejector refrigeration system with environmentally friendly working fluids from energy, conventional exergy and advanced exergy perspectives. Energ Convers Manage 2017;148:1208-24.

[35] Yang A, Shen WF, Wei SA, Dong LC, Li J, Gerbaud V. Design and Control of Pressure-Swing Distillation for Separating Ternary Systems with Three Binary Minimum Azeotropes. AIChE J 2019; 65(4):1281-93.

[36] Chen JY, Havtun H, Palm B. Conventional and advanced exergy analysis of an ejector refrigeration system. Appl Energy 2015;144:139-51.

[37] Li TL, Meng N, Liu J, Zhu JL, Kong XF. Thermodynamic and economic evaluation of the organic Rankine cycle (ORC) and two-stage series organic Rankine cycle (TSORC) for flue gas heat recovery. Energ Convers Manage 2019; 183:816-29.

[38] Bao J, Zhao L. A review of working fluid and expander selections for organic Rankine cycle. Renew Sustain Energy Rev 2013;24:325-42

[39] Hung T, Shai T, Wang S. A review of organic Rankine cycles (ORCs) for the recovery of low-grade waste heat. Energy 1997;22(7):661-7.

[40] Bao J, Zhao L. A review of working fluid and expander selections for organic Rankine cycle. Renew Sustain Energy Rev 2013;24(0):325-42

[41] Mago PJ, Chamra LM, Srinivasan K, Somayaji C. An examination of regenerative organic Rankine cycles using dry fluids. Appl Therm Eng 2008;28(8): 998-1007.

[42] Invernizzi C, Iora P, Silva P. Bottoming micro-Rankine cycles for micro-gas turbines. Appl Therm Eng 2007;27(1):100-110

[43] Xu J, Yu C. Critical temperature criterion for selection of working fluids for subcritical pressure Organic Rankine cycles. Energy 2014;74:719-33

[44] Tchanche BF, Papadakis G, Lambrinos G, Frangoudakis A. Fluid selection for alow-temperature solar organic Rankine cycle. Appl Therm Eng 2009; 29(11-12):2468-76

[45] Campanario FJ, Gutiérrez Ortiz FJ. Techno-economic assessment of bio-oil aqueous phase-to-liquids via Fischer-Tropsch synthesis and based on supercritical water reforming. Energy Convers Manage 2017;154:591-602.

[46] Galindo J, Climent H, Dolz V, Royo-Pascual L. Multi-objective optimization of a bottoming Organic Rankine Cycle ORC) of gasoline engine using swash-plate expander. Energy Convers Manage 2016;126:1054-65.

[47] Chacartegui R, Becerra JA., Blanco MJ, Muñoz-Escalona JM. A Humid Air Turbine–Organic Rankine Cycle combined cycle for distributed microgeneration. Energy Convers Manage 2015;104:115-26.

[48] Patel B, Desai NB, Kachhwaha SS. Optimization of waste heat based organic Rankine cycle powered cascaded vapor compression-absorption refrigeration system. Energy Convers Manage 2017;154:576-90.

[49] Yang A, Sun SR, Eslamimanesh A, Wei SA, Shen WF. Energy-saving investigation for diethyl carbonate synthesis through the reactive dividing wall column combining the vapor recompression heat pump or different pressure thermally coupled technique. Energy 2019;172:320-32.

[50] Shen WF, Dong LC, Wei SA, Li J, Benyounes H, You XQ, Gerbaud V. Systematic Design of Extractive Distillation for Maximum-boiling Azeotropes with Heavy Entrainers. AIChE J 2015; 61(11): 3898-910..

[51] Martelli E, Elsido C, Mian A, Marechal F. MINLP model and two-stage algorithm for the simultaneous synthesis of heat exchanger networks, utility systems and heat recovery cycles. Comput Chem Eng 2017;106:663-689.

[52] Luyben WL. Distillation Design and Control Using AspenTM Simulation. Hoboken, NJ,USA: John Wiley & Sons, Inc.; 2006. doi:10.1002/0471785253.